Published in final edited form as:
Cell Metab. 2009 April ; 9(4): 362–374. doi:10.1016/j.cmet.2009.03.005.

Critical role for hypothalamic mTOR activity in energy balance

Hiroyuki Mori[1,2], **Ken Inoki**[1], **Heike Münzberg**[3,*], **Darren Opland**[3,4], **Miro Faouzi**[3], **Eneida C. Villanueva**[2,3], **Tsuneo Ikenoue**[1], **David Kwiatkowski**[5], **Ormond A MacDougald**[2,3], **Martin G. Myers Jr.**[2,3,4,#], and **Kun-Liang Guan**[1,6,7,8,#]

[1] Life Sciences Institute, University of Michigan, Ann Arbor, Michigan 48109

[2] Department of Molecular and Integrative Physiology, University of Michigan, Ann Arbor, Michigan 48109

[3] Department of Medicine, University of Michigan, Ann Arbor, Michigan 48109

[4] Program in Neuroscience, University of Michigan, Ann Arbor, Michigan 48109

[6] Department of Biological Chemistry, University of Michigan, Ann Arbor, Michigan 48109

[7] Institute of Gerontology, University of Michigan, Ann Arbor, Michigan 48109

[5] Division of Translational Medicine, Department of Medicine, Brigham and Women's Hospital Harvard Medical School, Boston, Massachusetts 02115

[8] Department of Pharmacology and Moores Cancer Center, University of California San Diego, La Jolla, CA 92093-0815

Summary

The mammalian target of Rapamycin (mTOR) promotes anabolic cellular processes in response to growth factors and metabolic cues. The TSC1 and TSC2 tumor suppressors are major upstream inhibitory regulators of mTOR signaling. Mice with *Rip2*/*Cre*-mediated deletion of *Tsc1* (*Rip-Tsc1*cKO mice) developed hyperphagia and obesity, suggesting that hypothalamic disruption (for which *Rip2*/*Cre* is well known) of *Tsc1* may dysregulate feeding circuits via mTOR activation. Indeed, *Rip-Tsc1*cKO mice displayed increased mTOR signaling and enlarged neuron cell size in a number of hypothalamic populations, including Pomc neurons. Furthermore, *Tsc1* deletion with *Pomc*/Cre (*Pomc-Tsc1*cKO mice) resulted in dysregulation of Pomc neurons and hyperphagic obesity. Treatment with the mTOR inhibitor, rapamycin, ameliorated the hyperphagia, obesity, and the altered Pomc neuronal morphology in developing or adult *Pomc-Tsc1*cKO mice, and cessation of treatment reinstated these phenotypes. Thus, ongoing mTOR activation in Pomc neurons blocks the catabolic function of these neurons to promote nutrient intake and increased adiposity.

INTRODUCTION

The mammalian target of rapamycin (mTOR), an evolutionarily conserved serine-threonine kinase, promotes anabolic cellular processes such as protein synthesis in response to growth factors, nutrients (amino acids and glucose), and stress (Biondi et al., 2004; Wullschleger et al., 2006). mTOR exists in two distinct complexes, mTORC1 and mTORC2. TSC1 and TSC2

#Corresponding authors, Kun-Liang Guan (kuguan@ucsd.edu) and Martin G. Myers, Jr. (mgmyers@med.umich.edu).
*Present address: Pennington Biological Research Center, LSU System, Baton Rouge, LA.

are tumor suppressors and their gene products form a stable complex. The major function of TSC1/TSC2 tumor suppressors is to inhibit mTORC1 (Inoki et al., 2005), and mutation in either TSC1 or TSC2 leads to constitutive activation of mTORC1; in patients, this results in multi-organ hamartomas. The TSC1/TSC2 dimer has GTPase activating protein (GAP) activity specifically towards the Rheb GTPase, which directly binds and activates TORC1 but not TORC2 (Long et al., 2005; Sancak et al., 2007; Yang et al., 2006). Furthermore, amino acids and cellular energy levels stimulate TORC1, but not TORC2. For the purposes of this report, subsequent statements about mTOR refer to TORC1.

Within the TSC1/2 complex, the TSC1 subunit stabilizes and regulates the GAP activity of TSC2, which inactivates Rheb. During insulin signaling, the PI3K-Akt pathway activates mTOR by phosphorylating and thereby inhibiting TSC2 (Inoki et al., 2002; Manning et al., 2002; Nguyen et al., 2006); the Akt-dependent phosphorylation of PRAS40 may also contribute to mTOR activation (Oshiro et al., 2007; Sancak et al., 2007; Vander Haar et al., 2007; Wang et al., 2007). Energy limitation, such as glucose deprivation, strongly inhibits mTOR, and the glucose deprivation-induced mTOR inhibition is compromised in TSC mutant cells. AMPK, a cellular energy sensor, directly phosphorylates TSC2 to inhibit mTOR. AMPK can also inhibit mTORC1 by phosphorylating Raptor, an essential mTOR1 subunit. Thus, the TSC1/2 complex integrates multiple upstream signals to modulate mTOR activity (Gao et al., 2002; Inoki et al., 2003; Inoki et al., 2002; Manning et al., 2002; Wullschleger et al., 2006).

Although the PI3K-Akt cascade regulates many cellular processes by phosphorylating numerous substrates, including FOXO and AS160, and plays an important role in the hypothalamic control of feeding (Belgardt et al., 2008; Brunet et al., 1999; Kitamura et al., 2006; Kops et al., 1999; Plum et al., 2006; Sano et al., 2003), the function of mTOR activation for appetite regulation by the CNS has not been thoroughly investigated. Recent findings have suggested a potential role for mTOR as a cellular fuel sensor in hypothalamic circuits that regulate energy balance, especially in orexigenic AgRP-expressing neurons, where feeding status prominently regulates mTOR activity (Cota et al., 2006). Increased hypothalamic availability of leucine stimulates mTOR activity and reduces food intake in an mTOR-dependent manner. Hypothalamic mTOR activity is also required for the suppression of feeding by leptin. Thus, mTOR contributes to acute sensing of the nutritional milieu in the regulation of feeding by hypothalamic neural circuits. In contrast, the hyperactivation of mTOR in peripheral metabolic tissues such as muscle and liver during nutritional excess in high-calorie feeding and obesity also contributes to insulin resistance and metabolic dysfunction (Korsheninnikova et al., 2006; Miller et al., 2008). Such chronic activation of mTOR could similarly dysregulate the energy-sensing hypothalamic neurons that control feeding, and perturb whole body energy balance.

We generated mice conditionally lacking *Tsc1* in both pancreatic β cells and hypothalamic neurons (*Rip-Tsc1*cKO mice) using *Rip2/Cre*, and also lacking Tsc1 specifically in Pomc neurons *(Pomc-Tsc1*cKO*)* using *Pomc/Cre*. Our studies demonstrate hyperphagic obesity in both the *Rip-Tsc1*cKO and *Pomc-Tsc1*cKO mice, due to uncontrolled chronic activation of mTOR in both Rip neurons and Pomc neurons. These results suggest that the TSC-mTOR pathway plays crucial roles in the function of appetite-suppressing neural circuits; dysregulated activation of the mTOR pathway in the CNS might be a potential mechanism leading to the development of obesity.

RESULTS

Hyperphagic obesity in *Rip-Tsc1*cKO mice

To study the *in vivo* function of mTOR activation in metabolism, we set out to analyze mice lacking Tsc1, a major upstream negative regulator of mTOR. Since conventional knockout of

Tsc1 leads to embryonic lethality (Kobayashi et al., 2001; Kwiatkowski et al., 2002; Murakami et al., 2004), we generated a loxP-flanked floxed *Tsc1* allele ($Tsc1^{lox}$) to permit tissue specific *Tsc1* knockout. $Tsc1^{lox/lox}$ homozygotes (Meikle et al., 2005; Uhlmann et al., 2002) were mated with the *Cre* transgenic line driven by the rat insulin promoter 2 (Rip) (Choudhury et al., 2005; Kubota et al., 2004; Lin et al., 2004; Nguyen et al., 2006; Stiles et al., 2006). All subsequent experiments were performed using *Rip-cre*/$Tsc1^{lox/lox}$ (*Rip-Tsc1*cKO) mice and littermate $Tsc1^{lox/lox}$ (a.k.a. control/wild-type) mice. Western blotting confirmed markedly reduced *Tsc1* expression in isolated islets from *Rip-Tsc1*cKO mice (data not shown). As expected, *Tsc1* deletion mediated by *Rip*/*Cre* results in increased mTOR activity in β cells, along with increased β cell size and islet mass, and higher insulin content and secretion (Mori et. al unpublished observations).

Interestingly, in addition to their β cell phenotype, *Rip-Tsc1*cKO male mice displayed increased body weight compared with controls by 6 weeks of age (Figure 1A). By 12 weeks of age, *Rip-Tsc1*cKO mice were 36% heavier than control animals. The body weight of the *Rip-Tsc1*cKO female mice was also significantly higher than that of the controls (data not shown). Furthermore, 24 week-old *Rip-Tsc1*cKO mice displayed increased whole body fat content and increased adipocyte cell size compared with that of wild-type mice (Figure 1B, 1C). No difference in length was observed between the two genotypes (Supplementary Figure 1A). Consistent with the increased adiposity of *Rip-Tsc1*cKO mice, serum leptin levels were significantly elevated relative to controls in both fasted and fed states in *Rip-Tsc1*cKO mice at 4 weeks of age, at which the *Rip-Tsc1cKO* mice have normal body weight (Figure 1D). To examine leptin action in *Rip-Tsc1*cKO mice, we assessed the effect of administering leptin peripherally for 2 days. This treatment markedly reduced food intake and body weight in control animals (Figure 1E, 1F). In contrast, leptin had little effect on food intake in the *Rip-Tsc1*cKO mice, suggesting impairment of the leptin-regulated neural satiety circuits in these *Rip-Tsc1*cKO mice.

In order to understand the basis for this increased adiposity, we examined food intake from 4–6 weeks of age, when the difference in body weight between the two genotypes began to appear. We found that food consumption by *Rip-Tsc1*cKO mice was greater than that of the control animals (Figure 1G), suggesting that the obese phenotype in *Rip-Tsc1*cKO mice results from increased food intake. Consistently, pair-fed *Rip-Tsc1*cKO mice displayed similar body weights compared to wild-type mice (Figure 1H). Thus, *Rip-Tsc1*cKO mice develop hyperphagic obesity, suggesting an important role for mTOR in the regulation of food intake and body weight.

Hypothalamic *Tsc1* deletion in *Rip-Tsc1*cKO mice

Rip-Cre mice express Cre in the hypothalamus during development, resulting in the excision of floxed genes in a diverse set of hypothalamic neurons (Choudhury et al., 2005; Kubota et al., 2004; Lin et al., 2004; Nguyen et al., 2006; Stiles et al., 2006). Although immunoblotting revealed no detectable alteration in Tsc1 protein levels in the whole brain of *Rip-Tsc1*cKO mice (Supplementary Figure 1B), analysis of the dissected hypothalamus demonstrated reduced Tsc1 protein levels, supporting Cre-mediated deletion of *Tsc1* in the hypothalamus of these animals (Figure 2A). Tsc2 expression was also decreased when *Tsc1* was deleted (Figure 2A), consistent with the proposed role for Tsc1 in stabilizing Tsc2 (Chong-Kopera et al., 2006; Meikle et al., 2007). We determined the activation status of mTOR by immunoblotting for phosphorylated S6 (pS6). The mTOR-dependent activation of S6K results in S6 phosphorylation, which thus serves as a convenient readout for mTOR activity (Flotow and Thomas, 1992; Pende et al., 2004). Immunoblotting revealed markedly increased pS6 levels in the hypothalamus of *Rip-Tsc1*cKO mice (Figure 2A). Immunofluorescence analysis confirmed elevated pS6-immunoreactivity (pS6-IR) in many neurons in a number of

hypothalamic nuclei important for energy homeostasis (including the arcuate nucleus (ARC), ventromedial hypothalamic nucleus (VMH) and dorsomedial hypothalamic nucleus (DMH)), indicating that mTOR was activated in the hypothalamus of these animals (Figure 2B and Supplementary Figure 2). To test the mTOR-dependence of the increased pS6 in *Rip-Tsc1*cKO hypothalami, we treated the mice with rapamycin, a specific mTOR inhibitor. While not restored by the peripheral administration of 1mg/kg rapamycin (which ameliorated the effects of Tsc1 deletion in the β cell (Mori et. al unpublished data), higher (6 mg/kg) doses of rapamycin normalized pS6-IR in *Rip-Tsc1*cKO hypothalami, revealing the mTOR-dependency of the hypothalamic pS6 (Figure 2B).

Dysregulation of the melanocortin system in *Rip-Tsc1*cKO mice

The *Rip-Tsc1*cKO mice display high leptin levels and hyperphagia (Figure 1D, 1G). The inability of elevated leptin levels to mitigate hyperphagia in *Rip-Tsc1*cKO mice suggests the potential dysfunction of the neural systems that regulate body energy homeostasis in response to leptin in these animals. Quantitative real-time PCR (qPCR) analysis demonstrated that leptin receptor (*Lepr*) mRNA levels were increased in *Rip-Tsc1*cKO hypothalami (supplementary Figure 3), however, suggesting that the obesity of the *Rip-Tsc1*cKO animals was not due to attenuated *Lepr* expression. In order to identify potential contributing mechanisms underlying the altered feeding and energy balance of the *Rip-Tsc1*cKO mice, we examined mRNA expression of hypothalamic appetite-controlling neuropeptides that are known to be regulated by leptin (Coll et al., 2007; Flier, 2004). ARC neurons release orexigenic peptides, such as neuropeptide Y (NPY) and agouti-related peptide (AgRP), and anorexigenic peptides such as those derived from pro-opiomelanocortin (POMC). *Pomc* and *Npy* mRNA levels were dysregulated in *ad libitum*-fed *Rip-Tsc1*cKO mice, and fasting failed to decrease Npy mRNA levels in these mice; *Agrp* mRNA levels were normal and remained responsive to fasting in these animals (Figure 2C). Both increased *Npy* and decreased *Pomc* expression would predict increased feeding in the *Rip-Tsc1*cKO mice. The appropriate control of *Agrp* expression in the same neurons that display dysregulated *Npy* expression is consistent with previous findings demonstrating that the expression of *Npy* and *Agrp* are controlled by distinct upstream signals (Bates et al., 2003; Kitamura et al., 2006), and suggests an important role for hypothalamic mTOR in the regulation of *Npy*, but not *Agrp*. The dysregulation of neuropeptide expression in multiple populations of ARC neurons is consistent with *Rip2/Cre*-mediated deletion in multiple populations of hypothalamic neurons, including both anorectic and orexigenic cell types. Other neuronal populations are likely affected, as well, and the anorectic action of the majority of the neurons in this region of the hypothalamus presumably results in a net orexigenic response to the dysregulation of neurons throughout the ARC. These results suggest that uncontrolled mTOR activation blunts the physiological regulation of *Pomc* and *Npy* and that dysregulation of anorexigenic neurons, such as the Pomc cells, may contribute to the hyperphagic obesity of the *Rip-Tsc1*cKO mice.

We examined the somatic size and projections of the anorexigenic Pomc neurons by immunohistochemical analysis of ACTH, a neuropeptide derived from POMC. Visual inspection suggested the marked hypertrophy of ACTH-IR neuronal soma in the arcuate nucleus of the hypothalamus (ARC) (Figure 3A) along with the diminution of ACTH-IR neuronal projections to the PVN in *Rip-Tsc1c*KO mice compared to controls (Figure 3B). Thus ablation of Tsc1 by *Rip2*/*Cre* likely impairs signaling by Pomc neurons. In order to examine the mTOR-dependence of these effects, we treated animals with rapamycin for 2 weeks (from 2–4 weeks of age), using the dose (6 mg/kg, i.p.) that we had previously found effective in attenuating the increased hypothalamic mTOR activity in *Rip-Tsc1c*KO mice (Figure 2B). As shown in Figure 3A, this treatment largely corrected the obvious morphological alterations of ACTH-IR cells in the *Rip-Tsc1*cKO mice, as well as increasing the density of ACTH-IR projections to the PVN in *Rip-Tsc1*cKO mice (Figure 3B). Consistent with these histologic

improvements, the body weight phenotype of the Rapamycin-treated *Rip-Tsc1*cKO mice improved (Figure 3C).

Taken together, these data suggest a crucial role for Tsc1 in inhibiting mTOR activity and thereby preserving the normal regulation and function of hypothalamic neurons that modulate energy balance, and further suggest a potential contribution of pathologic changes promoted by mTOR activation in the Pomc neurons of the *Rip-Tsc1*cKO mice to the hyperphagic obesity of these animals.

Altered Pomc neurons in *Pomc-Tsc1*cKO mice

While the excision of conditional alleles in the hypothalamus by the *Rip2*/*Cre* transgene is well established, the neurons affected by this excision are diverse and poorly characterized, rendering it difficult to pinpoint a single neuronal mechanism underlying the obesity of *Rip-Tsc1*cKO mice. The alterations observed within the Pomc neurons of the *Rip-Tsc1*cKO mice suggest that these neurons represent one affected population and that mTOR activation in the Pomc neurons might contribute to the hyperphagic obesity of the *Rip-Tsc1*cKO mice, however. We thus generated mice harboring a conditional disruption of *Tsc1* specifically in Pomc neurons (*Pomc-Tsc1*cKO mice). The hypothalami of these *Pomc-Tsc1*cKO animals displayed elevated pS6-IR independent of nutritional status in a discrete set of enlarged ARC neurons (Figure 4A). While the rapid export of neuropeptides from the neural soma in mice prevents the detection of all Pomc neurons by ACTH-IR, the number of ACTH-IR neurons did not differ between *Pomc-Tsc1*cKO and control animals (Figure 4B, 4D left graph). The ACTH-IR Pomc soma colocalized with the pS6-IR neurons in the *Pomc-Tsc1*cKO animals, and the size of the ACTH-IR neurons was significantly increased in the *Pomc-Tsc1*cKO animals, consistent with the known specificity of Pomc/*Cre* for these neurons as well as the increased mTOR activity that accompanies the deletion of *Tsc1* (Figure 4B, 4D). The *Pomc-Tsc1*cKO mice also displayed decreased ACTH-IR axonal projections to the PVN (Figure 4C, 4D right graph) compared to control mice. Both the colocalization of strong pS6-IR in ACTH-IR neurons and the shift in the size of all ACTH-IR soma in the *Pomc-Tsc1*cKO mice (supplemental Figure 4A) suggests an efficient excision of *Tsc1* in these animals. Thus, mTOR activation cell-autonomously promotes hypertrophy in Pomc soma and abnormal ATCH-IR neuronal projections in *Pomc-Tsc1*cKO mice.

Hyperphagic obesity in *Pomc-Tsc1*cKO mice

We found that *Pomc-Tsc1*cKO mice weighed significantly more than control mice by 6 weeks of age (Figure 5A), and this increase in body weight reflected increased adiposity, as demonstrated by their increased fat pad mass and circulating leptin levels (Figure 5B, 5C, supplementary Figure 4C). To directly examine leptin action in *Pomc-Tsc1*cKO mice, we assessed the effect of administering leptin peripherally for 2 days. Though leptin treatment markedly reduced food intake and body weight in control animals, this effect was significantly attenuated in the *Pomc-Tsc1*cKO mice (Figure 5D, 5E). Furthermore, *Pomc-Tsc1*cKO mice consumed more food than controls during the period of highly divergent weight gain from 6–8 weeks of age (Figure 5F). These changes were not attributable to alterations in the HPA (hypothalamic-pituitary-adrenal) axis, as circulating corticosterone levels were similar in control and *Pomc-Tsc1*cKO animals at 4 and 24 weeks of age (supplementary Figure 4B). These data indicate that *Tsc1* ablation in Pomc neurons alone induced hyperphagic obesity. Taken together, our results suggest that TSC-mTOR signals in Pomc neurons play a crucial role in the physiology of these neurons and in the regulation of energy homeostasis, and that anabolic mTOR signaling in the Pomc neurons attenuates the catabolic function of these neurons to promote energy uptake and storage.

Rapamycin treatment of *Pomc-Tsc1*cKO mice

In order to examine roles for altered development and ongoing mTOR activity in the phenotypes of the *Pomc-Tsc1*cKO animals, we chronically treated two groups of animals with centrally effective doses of rapamycin (6 mg/kg, i.p.; see Figure 3B) or vehicle (Figure 6A, supplemental Figure 5A). In the first group (Treatment A), 2-week-old *Pomc-Tsc1*cKO and wild-type mice were treated with rapamycin for 5 weeks (from 2 to 7 weeks of age), and then switched to vehicle treatment for an additional 5 weeks (from 7 to 12 weeks of age). Conversely, for Treatment B, the animals were treated with vehicle for the initial 5 weeks, and then switched to rapamycin treatment for the second 5-week period. For each treatment group, some animals were sacrificed at 7 or 12 weeks of age for the analysis of fat pads and hypothalamic histology. We examined average food intake from 4–7 weeks of age and again after the switch in treatment from 7–12 weeks of age.

The body weight of *Pomc-Tsc1*cKO male mice was similar to controls during the rapamycin treatment period from 2–7 weeks of age in Treatment A, but the *Pomc-Tsc1*cKO mice gained significantly more weight following the switch to vehicle treatment after 7 weeks of age (Figure 6B upper). The adiposity (measured by fat pad weight), leptin levels, and food intake for the *Pomc-Tsc1*cKO mice was also similar to controls throughout the initial rapamycin treatment phase of these animals, but increased along with body weight following the switch to vehicle in Treatment A (Figure 6C–E). Thus, while rapamycin treatment from 2–7 weeks of age normalizes metabolic parameters in *Pomc-Tsc1*cKO mice, these improvements are lost upon discontinuation of rapamycin.

As for untreated animals (Figure 5), the body weight of *Pomc-Tsc1*cKO mice increased rapidly compared to controls in the first (vehicle treatment) phase of Treatment B animals (Figure 6B lower); these animals also displayed hyperphagia with increased fat pad weight and leptin levels (Figure 6C–E). The divergence in body weight between the *Pomc-Tsc1*cKO and control animals ceased upon the initiation of rapamycin treatment at 7 weeks of age, however, and food intake and measures of adiposity all decreased toward control levels during the second (rapamycin) phase of Treatment B (Figure 6B–E). Interestingly, hypothalamic *Pomc* mRNA expression did not vary by genotype, consistent with the mainly non-transcriptional function of mTOR, and suggesting that the altered *Pomc* mRNA expression noted in *Rip-Tsc1*cKO mice was likely due to indirect, rather than cell-autonomous effects of mTOR activation (Supplementary Figure 5B). Similarly, blood glucose levels did not vary among groups, nor were there differences in linear growth (as measured by snout to anus length) between genotypes under any treatment conditions, although this measure was slightly decreased by rapamycin treatment in both genotypes (Supplementary Figure 5C, 5D). Since genetic interference with central melanocortin action generally promotes increased linear growth, the normal body length of the *Pomc-Tsc1*cKO mice suggests that cell-autonomous mTOR activation interferes with other important aspects of Pomc neuron action.

Thus, the physiologic phenotypes of animals subjected to Treatment A and Treatment B animals suggest an important role for ongoing mTOR activation (as opposed to mTOR-mediated alterations in development) in the hyperphagia and obesity of *Pomc-Tsc1*cKO mice, since mTOR blockade normalizes the metabolism of adult as well as younger animals, and since these changes are reversed when mTOR inhibition ceases.

Rapamycin normalizes neuronal morphology in *Pomc-Tsc1*cKO mice

In order to examine the potential alteration of Pomc neurons with mTOR activation and rapamycin-mediated inhibition, we examined the size of Pomc neurons and the density of Pomc projections to the PVN by ACTH immunofluorescence in 7 and 12 week-old animals subjected to Treatment A and Treatment B. While rapamycin treatment from 2–7 weeks of Treatment A

normalized the size of Pomc soma and the density of PVN projections in the *Pomc-Tsc1*cKO mice at 7 weeks of age (Figure 7A, 7B), the size of these neurons increased and their projection density decreased over the subsequent 5 weeks of vehicle treatment (Figure 7A, 7B). While the size of Pomc neurons in vehicle-treated *Pomc-Tsc1*cKO mice was increased and PVN projections were decreased relative to controls at 7 weeks of age (Figure 7A, 7B), rapamycin administration to these animals from 7–12 weeks significantly reduced their Pomc somatic size and partially improved the detection of ACTH-IR PVN projections in Treatment B (Figure 7A, 7B). Thus, the increased size of Pomc neurons and their decreased projection density to the PVN in *Pomc-Tsc1*cKO mice is preventable by mTOR inhibition in young animals, but reverts upon the cessation of treatment. While the alterations in Pomc somatic size remain largely reversible by mTOR inhibition in older animals, rapamycin administration to these adult animals does not completely restore ACTH-IR PVN projections, suggesting roles for mTOR activity both in the development and in the ongoing regulation of these projections. In contrast, the ongoing levels of mTOR activity, not developmental processes, largely determine the somatic size of Pomc neurons and metabolic parameters in *Pomc-Tsc1*cKO mice.

DISCUSSION

The data presented here suggest that the hyperphagic and obese phenotype of *Rip-Tsc1*cKO mice likely results from the ablation of *Tsc1* in the hypothalamus. Indeed, the β-cell specific (without hypothalamic involvement) knockout of *Tsc2* caused hyperinsulinemia but not obesity (Shigeyama et al., 2008). Furthermore, treatment of mice with low dose rapamycin (1mg/kg body weight), which blocks β-cell hypertrophy and hyperinsulinemia but does not normalize hypothalamic pS6-IR, does not prevent the hyperphagia and obesity of the *Rip-Tsc1*cKO mice (Mori et al., unpublished observations).

Deletion of *Tsc1* specifically from Pomc-expressing cells results in hyperphagia and obesity in *Pomc-Tsc1*cKO mice, and this phenotype cannot be attributed to alterations in the function of pituitary corticotrophs. Thus, these data suggest that constitutive activation of mTOR in anorexigenic neurons of the hypothalamus dysregulates these neurons and results in hyperphagic obesity. These neurons respond to a variety of signals, including leptin and nutrients, to decrease feeding. A variety of data also suggest an important role for the insulin signaling cascade (including PI3-kinase) in the regulation of neuronal activity and metabolism (Belgardt et al., 2008; Choudhury et al., 2005; Kubota et al., 2004; Lin et al., 2004; Plum et al., 2006). While the activation of mTOR in peripheral tissues interferes with insulin/PI3-kinase signaling, we were not able to detect alterations in PI3-kinase signaling in the *Pomc-Tsc1*cKO mice (data not shown). The anorectic response to central insulin is modest, and most inactivating mutations in insulin signaling molecules (e.g., Insulin Receptor, PI3-kinase, IRS-proteins, etc.) in POMC neurons produce little change in overall energy balance (Hill et al., 2008; Choudhury et al., 2005; Belgardt et al., 2008; Konner et al., 2007). These findings, along with the dramatic obesity of the *Pomc-Tsc1*cKO animals, suggest that a direct effect of mTOR activation, rather than interference with PI3-kinase, underlies the obesity of *Pomc-Tsc1*cKO mice.

Increased mTOR activity cell-autonomously increases the somatic size of Pomc neurons, consistent with the hypertrophic effects of mTOR in other tissues (Meikle et al., 2008; Rachdi et al., 2008; Shigeyama et al., 2008). Increased cell-autonomous mTOR activity also impairs the ACTH-IR projections from the ARC Pomc neurons. mTOR activation appears to modulate the detection of ACTH-IR PVN projections by developmental as well as ongoing processes, since the normalization of projections by rapamycin treatment during development is at least partially reversed upon the cessation of treatment, and 5 weeks of treatment in older animals does not completely normalize projections in *Pomc-Tsc1*cKO mice. The detection of PVN projections by neuropeptide staining necessarily reflects the expression and axonal content of

the neuropeptide, and our data thus reflect the combination of ACTH-IR peptide content as well as the density of axonal projections to the PVN.

Increased Pomc somatic size in *Pomc-Tsc1*cKO mice is not developmentally programmed, but modulated by ongoing mTOR activity, as is the impaired catabolic action of the melanocortin system in these mice. These data reveal an important role for the post-developmental activation of mTOR in Pomc neurons for metabolic regulation. Note, however, that these data cannot rule out the possibility of a more modest effect of mTOR-dependent developmental alterations in the Pomc system on energy homeostasis, but rather reveal the dominant effect of ongoing mTOR activation in this model system. It is possible that the early activation of mTOR in Pomc and other hypothalamic neurons may alter their normal developmental program, as observed in states of maternal obesity and diabetes. Indeed, ablation of *Tsc1* in most neurons using *Synapsin-Cre* mice (*Syn-Tsc1*cKO) results in a variety of neuropathological abnormalities, including ectopic and hypomyelinated projections that may result from developmental abnormalities (Meikle et al., 2007).

In contrast to our present data demonstrating that long-term activation of the TSC-mTOR pathway impairs the function of anorectic Pomc neurons, Cota et al. showed that the acute pharmacologic inhibition of mTOR throughout the hypothalamus impairs appetite control-presumably at least in part via the regulation of AgRP neurons (Cota et al., 2006). A number of differences between these studies may underlie the distinct results obtained. While the Cota study essentially examined the effect of intracerebroventricular rapamycin in all hypothalamic (and presumably other) neurons near the 3rd cerebral ventricle, our study isolated the effect of mTOR activation specifically in Pomc neurons. Furthermore, as our unpublished data reveal that neuronal activity cell-autonomously regulates mTOR signaling in hypothalamic neurons (Villanueva and Myers in preparation), the function of hypothalamic mTOR in the ultimate regulation of appetite should depend upon the specific regulation and role of mTOR activity in each neural subtype. As importantly, our examination of a system with chronic activation of mTOR signaling contrasts with the acute mTOR inhibition strategy utilized by Cota, et al. Thus, in our genetic model, the chronic activation of mTOR in anorexigenic hypothalamic neurons may mimic the effects observed in the peripheral tissues of patients and animal models with obesity and type 2 diabetes.

Our study indicates that uncontrolled mTOR activity impairs the development of neuronal projections in a cell-autonomous manner. In contrast, the main effects of mTOR activation in Pomc neurons on somatic size and energy balance are reversible, and chronic ongoing activation of mTOR in the hypothalamic Pomc neurons, such as might be caused by overnutrition, promotes the development of hyperphagic obesity. Such dysregulation may promote hypothalamic dysfunction and further overeating in states of overnutrition and obesity.

MATERIALS AND METHODS

Animals and animal care

Tsc1$^{lox/lox}$ mice, with exons 17 and 18 of *Tsc1* flanked by loxP sites by homologous recombination have been described (Meikle et al., 2005; Uhlmann et al., 2002). We generated β cell and hypothalamic specific Tsc1 knockout mice (*Rip-Tsc1*cKO) by breeding *Tsc1*$^{lox/lox}$ mice with mice that express the *Cre* recombinase gene under the control of the rat insulin 2 gene promoter (The Jackson Laboratory). Mice were maintained on the mixed genetic background (C57Bl/6 × 129Sv × BALB/c). We performed experiments using *Rip-Cre*/*Tsc1*$^{lox/lox}$ (*Rip-Tsc1*cKO) mice and littermates *Tsc1*$^{lox/lox}$ as control (wild-type). *Pomc-Cre* mice (FVB background) from The Jackson Laboratory were mated with *Tsc1*$^{lox/lox}$ mice to generate *Pomc-Tsc1*cKO same as *Rip-Tsc1*cKO, and were maintained on mix genetic background. Mice were housed on a 12-hour light/12-hour dark cycle in the Unit for Laboratory

Animal Medicine (ULAM) at the University of Michigan, with free access to water and standard mouse chow. Animal experiments were conducted following protocols approved by the University Committee on the Use and Care of Animals (UCUCA).

In vivo physiological studies

Blood glucose levels were determined using an automated blood glucose reader (Accu-Check, Roche). Serum insulin and leptin levels were measured by ELISA (Crystal Chem, IL). For a leptin administration study, mice were individually caged. Murine leptin (PeproTech) (2.5mg/kg body weight) was injected intraperitoneally twice daily (at 09:00 and 18:00) for 2 days. Body weight and food intake were measured daily before injection, during the treatment period, and 2-day wash-out period following the injection. Serum corticosterone levels were measured by Hormone Assay & Analytical Services Core, MMPC, Vanderbilt University (NIH grant # DK59637).

Total body fat content was determined using a dual energy X-ray absorptiometry (DEXA) scanner (GE Medical Systems Lunar) according to the manufacturer's instructions.

Rapamycin treatment studies

Rapamycin (LC laboratories) was initially dissolved in 100% ethanol, stored at −20 °C, and further diluted in an aqueous solution of 5.2% Tween 80 and 5.2% PEG 400 (final ethanol concentration, 2%) immediately before use (Wendel et al., 2004). *Rip-Tsc1*cKO, *Pomc-Tsc1*cKO and their control animals were injected rapamycin intraperitoneally (6 mg/kg body weight, every other day) for the periods shown in the each experiment. Both pancreas and brain tissues for WB, RT-PCR and IHC were harvested after 12hr of the last treatment of rapamycin.

Immunohistochemistry

The Brains were harvested from both 24-hr-fasted or *ad libitum* fed mice at the beginning of light cycle. After transcardiac perfusion with 4% paraformaldehyde, brains were postfixed in 4% paraformaldehyde, then transferred to 20% sucrose solution for overnight. Tissues were frozen on dry ice and cut into 25-μm coronal sections on a sliding microtome, collected in 5 series, and stored in antifreeze solution (50% PBS, 15% ethyl glycol, and 35% glycerol) at −20°C until further use. One series of brain sections was then stained with Phospho-S6 (Ser235/236(IHC preferred) or Alexa Fluor 488 Conjugated; Cell Signaling Technology), and ACTH antibody (from Dr. Parwlow, NATIONAL HORMONE and PEPTIDE PROGRAM), using free-floating method.

Quantification of ATCH-positive cell size in the ARC and projections to the PVN

For quantification of cell size in ACTH positive cells in the ARC and projections to the PVN, we used ImageJ software (NIH, Bethesda MD). All high magnification images were converted into binary files using a unique threshold value that separated positively labeled cells from background. In order to exclude false positives, the average size of cells that fell within a strict set of parameters (larger than 0.2 μm^2 and between 0.50–1.00 circularity) was quantified. Average cell size of ACTH(+) cells within matched sections of the ARC were compared. For projection density measurements in the PVN, ACTH(+) stained slices were converted into binary files to separate labeled projections from background tissue. All images for intercomparison in this manner were collected using identical microscope and camera settings on tisse samples processed in parallel. Optical density measurements of projections within a 2.0×2.0 sized circular selection area placed over the left side of each PVN were compared.

Western blot analysis

Tissue extracts were immunoblotted with Tsc1, Tsc2, phospho-S6, S6 (Cell Signaling) and α-Tubulin (Sigma Aldrich).

mRNA quantification by RT-PCR analysis

Hypothalami were harvested immediately from both 24-hr-fasted and *ad libitum* fed mice at the beginning of light cycle, homogenized in Trizol reagent (Invitrogen). Total RNA was isolated and used for reverse transcription by SuperScript First-Strand Synthesis System (Invitrogen). Quantitative PCR was carried out with specific primers. *Leptin receptor* (*Lepr*), *Npy*, *Pomc*, *Agrp*, *hypoxanthine phosphoribosyltransferase 1* (*Hprt*) mRNA levels were measured using the ABI Prism 7300 Real-Time PCR System, with SYBR green reagents (Applied Biosystems Inc.). The expression of each mRNA level was normalized to the expression of *Hprt*. Primers for real-time RT-PCR were: *Lepr* sense 5′-GGGTTTATCCATAGTCCTGTCA-3′, *Lepr* antisense 5′-AAATGTCTGGGCCTCTGTCTCC-3′, *Hprt* sense 5′-TCATTATGCCGAGGATTTGGA-3′, *Hprt* antisense 5′-GCACACAGAGGGCCACAAT-3′. Primers for *Pomc*, *Npy*, *Agrp* were described previously (Bates et al., 2003).

Statistical analyses

All data are presented as mean ± s.e.m. and were analyzed by Student's *t*-test or analyses of variance (ANOVA). The differences were considered to be significant if $P < 0.05$.

Supplementary Material

Refer to Web version on PubMed Central for supplementary material.

Acknowledgments

This work was supported by grants from NIH and DOD (K.L.G), NIH DK57768 and DK56731 (MGM), DK51563 and DK62876 (OAM) and an AHA SDG to H. Mü; H. Mo was supported by the Uehara Memorial Foundation and a mentor-based postdoctoral fellowship from ADA. We thank Marta Dzaman, Wanda Snead, Chris Edwards, for technical advice and assistance, members of the Guan, MacDougald and Myers lab for helpful discussions and assistance.

References

Bates SH, Stearns WH, Dundon TA, Schubert M, Tso AW, Wang Y, Banks AS, Lavery HJ, Haq AK, Maratos-Flier E, Neel BG, Schwartz MW, Myers MG Jr. STAT3 signalling is required for leptin regulation of energy balance but not reproduction. Nature 2003;421:856–859. [PubMed: 12594516]

Belgardt BF, Husch A, Rother E, Ernst MB, Wunderlich FT, Hampel B, Klockener T, Alessi D, Kloppenburg P, Bruning JC. PDK1 deficiency in POMC-expressing cells reveals FOXO1-dependent and -independent pathways in control of energy homeostasis and stress response. Cell Metab 2008;7:291–301. [PubMed: 18396135]

Biondi CA, Gartside MG, Waring P, Loffler KA, Stark MS, Magnuson MA, Kay GF, Hayward NK. Conditional inactivation of the MEN1 gene leads to pancreatic and pituitary tumorigenesis but does not affect normal development of these tissues. Molecular and cellular biology 2004;24:3125–3131. [PubMed: 15060136]

Brunet A, Bonni A, Zigmond MJ, Lin MZ, Juo P, Hu LS, Anderson MJ, Arden KC, Blenis J, Greenberg ME. Akt promotes cell survival by phosphorylating and inhibiting a Forkhead transcription factor. Cell 1999;96:857–868. [PubMed: 10102273]

Chong-Kopera H, Inoki K, Li Y, Zhu T, Garcia-Gonzalo FR, Rosa JL, Guan KL. TSC1 stabilizes TSC2 by inhibiting the interaction between TSC2 and the HERC1 ubiquitin ligase. The Journal of biological chemistry 2006;281:8313–8316. [PubMed: 16464865]

Choudhury AI, Heffron H, Smith MA, Al-Qassab H, Xu AW, Selman C, Simmgen M, Clements M, Claret M, Maccoll G, Bedford DC, Hisadome K, Diakonov I, Moosajee V, Bell JD, Speakman JR, Batterham RL, Barsh GS, Ashford ML, Withers DJ. The role of insulin receptor substrate 2 in hypothalamic and beta cell function. The Journal of clinical investigation 2005;115:940–950. [PubMed: 15841180]

Coll AP, Farooqi IS, O'Rahilly S. The hormonal control of food intake. Cell 2007;129:251–262. [PubMed: 17448988]

Cota D, Proulx K, Smith KA, Kozma SC, Thomas G, Woods SC, Seeley RJ. Hypothalamic mTOR signaling regulates food intake. Science 2006;312:927–930. [PubMed: 16690869]

Flier JS. Obesity wars: molecular progress confronts an expanding epidemic. Cell 2004;116:337–350. [PubMed: 14744442]

Flotow H, Thomas G. Substrate recognition determinants of the mitogen-activated 70K S6 kinase from rat liver. The Journal of biological chemistry 1992;267:3074–3078. [PubMed: 1737763]

Gao X, Zhang Y, Arrazola P, Hino O, Kobayashi T, Yeung RS, Ru B, Pan D. Tsc tumour suppressor proteins antagonize amino-acid-TOR signalling. Nat Cell Biol 2002;4:699–704. [PubMed: 12172555]

Hill JW, Williams KW, Ye C, Luo J, Balthasar N, Coppari R, Cowley MA, Cantley LC, Lowell BB, Elmquist JK. Acute effects of leptin require PI3K signaling in hypothalamic proopiomelanocortin neurons in mice. The Journal of clinical investigation 2008;118:1796–1805. [PubMed: 18382766]

Inoki K, Corradetti MN, Guan KL. Dysregulation of the TSC-mTOR pathway in human disease. Nat Genet 2005;37:19–24. [PubMed: 15624019]

Inoki K, Li Y, Xu T, Guan KL. Rheb GTPase is a direct target of TSC2 GAP activity and regulates mTOR signaling. Genes Dev 2003;17:1829–1834. [PubMed: 12869586]

Inoki K, Li Y, Zhu T, Wu J, Guan KL. TSC2 is phosphorylated and inhibited by Akt and suppresses mTOR signalling. Nat Cell Biol 2002;4:648–657. [PubMed: 12172553]

Kitamura T, Feng Y, Kitamura YI, Chua SC Jr, Xu AW, Barsh GS, Rossetti L, Accili D. Forkhead protein FoxO1 mediates Agrp-dependent effects of leptin on food intake. Nat Med 2006;12:534–540. [PubMed: 16604086]

Kobayashi T, Minowa O, Sugitani Y, Takai S, Mitani H, Kobayashi E, Noda T, Hino O. A germ-line Tsc1 mutation causes tumor development and embryonic lethality that are similar, but not identical to, those caused by Tsc2 mutation in mice. Proceedings of the National Academy of Sciences of the United States of America 2001;98:8762–8767. [PubMed: 11438694]

Konner AC, Janoschek R, Plum L, Jordan SD, Rother E, Ma X, Xu C, Enriori P, Hampel B, Barsh GS, Kahn CR, Cowley MA, Ashcroft FM, Bruning JC. Insulin Action in AgRP-Expressing Neurons Is Required for Suppression of Hepatic Glucose Production. Cell Metab 2007;5:438–449. [PubMed: 17550779]

Kops GJ, de Ruiter ND, De Vries-Smits AM, Powell DR, Bos JL, Burgering BM. Direct control of the Forkhead transcription factor AFX by protein kinase B. Nature 1999;398:630–634. [PubMed: 10217147]

Korsheninnikova E, van der Zon GC, Voshol PJ, Janssen GM, Havekes LM, Grefhorst A, Kuipers F, Reijngoud DJ, Romijn JA, Ouwens DM, Maassen JA. Sustained activation of the mammalian target of rapamycin nutrient sensing pathway is associated with hepatic insulin resistance, but not with steatosis, in mice. Diabetologia 2006;49:3049–3057. [PubMed: 17006666]

Kubota N, Terauchi Y, Tobe K, Yano W, Suzuki R, Ueki K, Takamoto I, Satoh H, Maki T, Kubota T, Moroi M, Okada-Iwabu M, Ezaki O, Nagai R, Ueta Y, Kadowaki T, Noda T. Insulin receptor substrate 2 plays a crucial role in beta cells and the hypothalamus. The Journal of clinical investigation 2004;114:917–927. [PubMed: 15467830]

Kwiatkowski DJ, Zhang H, Bandura JL, Heiberger KM, Glogauer M, el-Hashemite N, Onda H. A mouse model of TSC1 reveals sex-dependent lethality from liver hemangiomas, and up-regulation of p70S6 kinase activity in Tsc1 null cells. Hum Mol Genet 2002;11:525–534. [PubMed: 11875047]

Lin X, Taguchi A, Park S, Kushner JA, Li F, Li Y, White MF. Dysregulation of insulin receptor substrate 2 in beta cells and brain causes obesity and diabetes. The Journal of clinical investigation 2004;114:908–916. [PubMed: 15467829]

Long X, Lin Y, Ortiz-Vega S, Yonezawa K, Avruch J. Rheb binds and regulates the mTOR kinase. Curr Biol 2005;15:702–713. [PubMed: 15854902]

Manning BD, Tee AR, Logsdon MN, Blenis J, Cantley LC. Identification of the tuberous sclerosis complex-2 tumor suppressor gene product tuberin as a target of the phosphoinositide 3-kinase/akt pathway. Molecular cell 2002;10:151–162. [PubMed: 12150915]

Meikle L, McMullen JR, Sherwood MC, Lader AS, Walker V, Chan JA, Kwiatkowski DJ. A mouse model of cardiac rhabdomyoma generated by loss of Tsc1 in ventricular myocytes. Hum Mol Genet 2005;14:429–435. [PubMed: 15601645]

Meikle L, Pollizzi K, Egnor A, Kramvis I, Lane H, Sahin M, Kwiatkowski DJ. Response of a neuronal model of tuberous sclerosis to mammalian target of rapamycin (mTOR) inhibitors: effects on mTORC1 and Akt signaling lead to improved survival and function. J Neurosci 2008;28:5422–5432. [PubMed: 18495876]

Meikle L, Talos DM, Onda H, Pollizzi K, Rotenberg A, Sahin M, Jensen FE, Kwiatkowski DJ. A mouse model of tuberous sclerosis: neuronal loss of Tsc1 causes dysplastic and ectopic neurons, reduced myelination, seizure activity, and limited survival. J Neurosci 2007;27:5546–5558. [PubMed: 17522300]

Miller AM, Brestoff JR, Phelps CB, Berk EZ, Reynolds THt. Rapamycin does not improve insulin sensitivity despite elevated mammalian target of rapamycin complex 1 activity in muscles of ob/ob mice. American journal of physiology 2008;295:R1431–1438. [PubMed: 18768766]

Murakami M, Ichisaka T, Maeda M, Oshiro N, Hara K, Edenhofer F, Kiyama H, Yonezawa K, Yamanaka S. mTOR is essential for growth and proliferation in early mouse embryos and embryonic stem cells. Molecular and cellular biology 2004;24:6710–6718. [PubMed: 15254238]

Nguyen KT, Tajmir P, Lin CH, Liadis N, Zhu XD, Eweida M, Tolasa-Karaman G, Cai F, Wang R, Kitamura T, Belsham DD, Wheeler MB, Suzuki A, Mak TW, Woo M. Essential role of Pten in body size determination and pancreatic beta-cell homeostasis in vivo. Molecular and cellular biology 2006;26:4511–4518. [PubMed: 16738317]

Oshiro N, Takahashi R, Yoshino K, Tanimura K, Nakashima A, Eguchi S, Miyamoto T, Hara K, Takehana K, Avruch J, Kikkawa U, Yonezawa K. The proline-rich Akt substrate of 40 kDa (PRAS40) is a physiological substrate of mammalian target of rapamycin complex 1. The Journal of biological chemistry 2007;282:20329–20339. [PubMed: 17517883]

Pende M, Um SH, Mieulet V, Sticker M, Goss VL, Mestan J, Mueller M, Fumagalli S, Kozma SC, Thomas G. S6K1(−/−)/S6K2(−/−) mice exhibit perinatal lethality and rapamycin-sensitive 5′-terminal oligopyrimidine mRNA translation and reveal a mitogen-activated protein kinase-dependent S6 kinase pathway. Molecular and cellular biology 2004;24:3112–3124. [PubMed: 15060135]

Plum L, Ma X, Hampel B, Balthasar N, Coppari R, Munzberg H, Shanabrough M, Burdakov D, Rother E, Janoschek R, Alber J, Belgardt BF, Koch L, Seibler J, Schwenk F, Fekete C, Suzuki A, Mak TW, Krone W, Horvath TL, Ashcroft FM, Bruning JC. Enhanced PIP3 signaling in POMC neurons causes KATP channel activation and leads to diet-sensitive obesity. The Journal of clinical investigation 2006;116:1886–1901. [PubMed: 16794735]

Rachdi L, Balcazar N, Osorio-Duque F, Elghazi L, Weiss A, Gould A, Chang-Chen KJ, Gambello MJ, Bernal-Mizrachi E. Disruption of Tsc2 in pancreatic beta cells induces beta cell mass expansion and improved glucose tolerance in a TORC1-dependent manner. Proceedings of the National Academy of Sciences of the United States of America 2008;105:9250–9255. [PubMed: 18587048]

Sancak Y, Thoreen CC, Peterson TR, Lindquist RA, Kang SA, Spooner E, Carr SA, Sabatini DM. PRAS40 is an insulin-regulated inhibitor of the mTORC1 protein kinase. Molecular cell 2007;25:903–915. [PubMed: 17386266]

Sano H, Kane S, Sano E, Miinea CP, Asara JM, Lane WS, Garner CW, Lienhard GE. Insulin-stimulated phosphorylation of a Rab GTPase-activating protein regulates GLUT4 translocation. The Journal of biological chemistry 2003;278:14599–14602. [PubMed: 12637568]

Shigeyama Y, Kobayashi T, Kido Y, Hashimoto N, Asahara S, Matsuda T, Takeda A, Inoue T, Shibutani Y, Koyanagi M, Uchida T, Inoue M, Hino O, Kasuga M, Noda T. Biphasic response of pancreatic beta-cell mass to ablation of tuberous sclerosis complex 2 in mice. Molecular and cellular biology 2008;28:2971–2979. [PubMed: 18316403]

Stiles BL, Kuralwalla-Martinez C, Guo W, Gregorian C, Wang Y, Tian J, Magnuson MA, Wu H. Selective deletion of Pten in pancreatic beta cells leads to increased islet mass and resistance to STZ-induced diabetes. Molecular and cellular biology 2006;26:2772–2781. [PubMed: 16537919]

Uhlmann EJ, Wong M, Baldwin RL, Bajenaru ML, Onda H, Kwiatkowski DJ, Yamada K, Gutmann DH. Astrocyte-specific TSC1 conditional knockout mice exhibit abnormal neuronal organization and seizures. Ann Neurol 2002;52:285–296. [PubMed: 12205640]

Vander Haar E, Lee SI, Bandhakavi S, Griffin TJ, Kim DH. Insulin signalling to mTOR mediated by the Akt/PKB substrate PRAS40. Nat Cell Biol 2007;9:316–323. [PubMed: 17277771]

Wang L, Harris TE, Roth RA, Lawrence JC Jr. PRAS40 regulates mTORC1 kinase activity by functioning as a direct inhibitor of substrate binding. The Journal of biological chemistry 2007;282:20036–20044. [PubMed: 17510057]

Wendel HG, De Stanchina E, Fridman JS, Malina A, Ray S, Kogan S, Cordon-Cardo C, Pelletier J, Lowe SW. Survival signalling by Akt and eIF4E in oncogenesis and cancer therapy. Nature 2004;428:332–337. [PubMed: 15029198]

Wullschleger S, Loewith R, Hall MN. TOR signaling in growth and metabolism. Cell 2006;124:471–484. [PubMed: 16469695]

Yang Q, Inoki K, Kim E, Guan KL. TSC1/TSC2 and Rheb have different effects on TORC1 and TORC2 activity. Proceedings of the National Academy of Sciences of the United States of America 2006;103:6811–6816. [PubMed: 16627617]

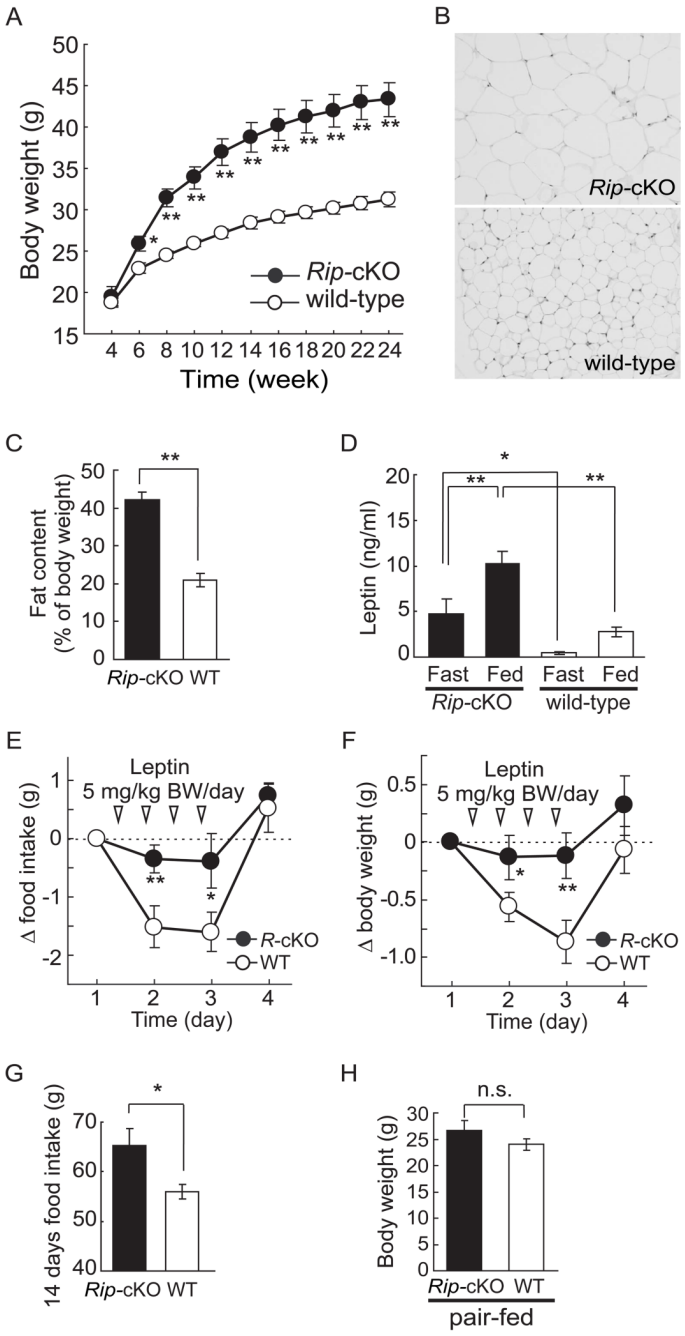

Figure 1. Hyperphagic obesity in *Rip-Tsc1*cKO mice

(**A**) Obesity in *Rip-Tsc1*cKO mice. Body weight in male littermates fed on regular chow diet from 4 to 24 weeks of age (n = 17–22).

(**B**) Increased adipocyte size in *Rip-Tsc1*cKO mice. H&E staining of epididymal fat depots from *Rip-Tsc1*cKO and control mice at 24-weeks of age.

(**C**) Increase of fat content in *Rip-Tsc1*cKO mice. Fat content was measured using a dual energy X-ray absorptiometry (DEXA) scanner (n = 6–7).

(**D**) Hyperleptinemia in *Rip-Tsc1*cKO mice. Serum leptin levels in 16 hr fasted or *ad lib* fed male mice at 4 weeks of age (n = 6–8).

(**E, F**) Impaired response to leptin in *Rip-Tsc1*cKO mice. Male mice at 4–5 weeks of age were injected intraperitoneally with leptin (2.5 mg/kg body weight) twice daily (at 09:30 and 18:30) for 2 days ($n = 6$). (**E**) Food intake was measured each day, and changes in food intake are reported relative to baseline intake. (**F**) Body weight was measured every day, and changes are reported relative to initial body weight.

(**G**) *Rip-Tsc1*cKO mice are hyperphagic. Food intake in 4-week-old male mice over a 2-week period ($n = 7–8$).

(**H**) Body weight of 8-week old pair-fed male mice. *Rip-Tsc1*cKO and wild-type mice were given the average amount of food consumed by age-matched control mice from 4 weeks of age 8 weeks of age ($n = 7$).

For panels (**A**)–(**H**), *Rip*-cKO or *R*-cKO:*Rip-Tsc1*cKO**,** WT: control, values are mean ± s.e.m. *$p<0.05$, **$p<0.001$

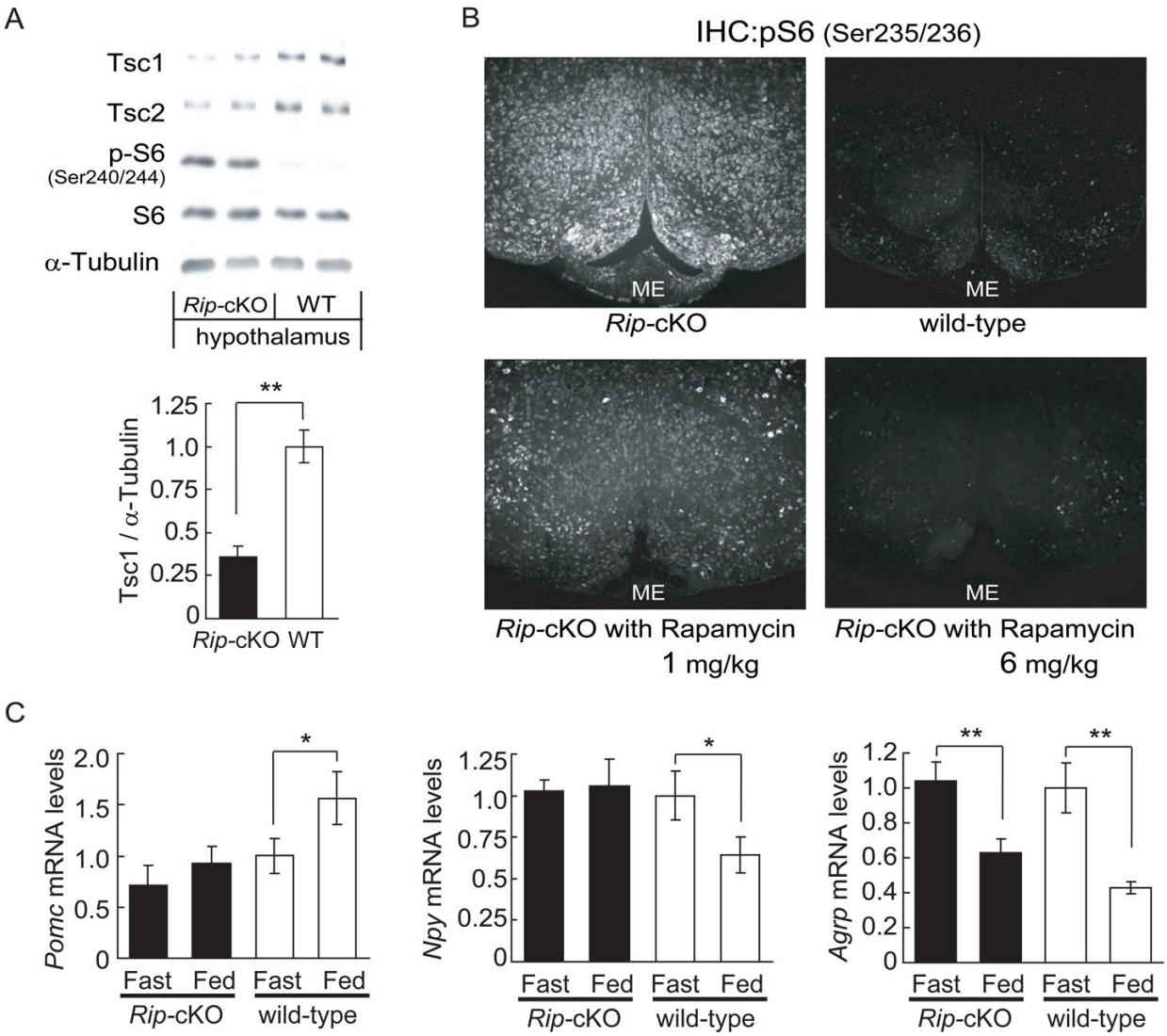

Figure 2. Hypothalamic *Tsc1* deletion and dysregulation of the melanocortin system in *Rip-Tsc1*cKO mice

(**A**) Tsc1 and Tsc2 protein levels decrease in *Rip-Tsc1*cKO hypothalamus. (Upper panel): Immunoblot analysis of Tsc1, Tsc2, p-S6, S6 and a α-Tubulin in the hypothalamus. Hypothalamic extracts were prepared from individual animals. (Lower panel): Amount of Tsc1 normalized to total α-Tubulin (n = 12).

(**B**) Elevated pS6-immunoreactivity (IR) in *Rip-Tsc1*cKO hypothalamus. Hypothalamic sections from *ad libitum* fed *Rip-Tsc1*cKO and control mice at 4-week ages were stained with p-S6 (Ser235/236) antibody. For rapamycin treatment, 2-week-old *Rip-Tsc1*cKO mice were injected with rapamycin (1mg/kg body weight) or high dose rapamycin (6mg/kg body weight), as indicated, every other day for two weeks. Hypothalami were harvested 12hr after the last treatment of rapamycin. ME: median eminence

(**C**) Altered expression of hypothalamic peptides in *Rip-Tsc1*cKO mice. *Pomc*, *Npy* and *Agrp* mRNA levels in the hypothalamus were measured by real time RT-PCR in 4 week old *Rip-Tsc1*cKO and control mice under 24-hr fasting and *ad lib* feeding conditions. Values normalized to *Hprt* mRNA are expressed relative to fasted control mice.

For panels (**A**), (**C**), data are expressed as the average ±s.e.m, **P* <0.05, ***P* <0.01. For all panels *Rip*-cKO: *Rip-Tsc1*cKO, WT: control.

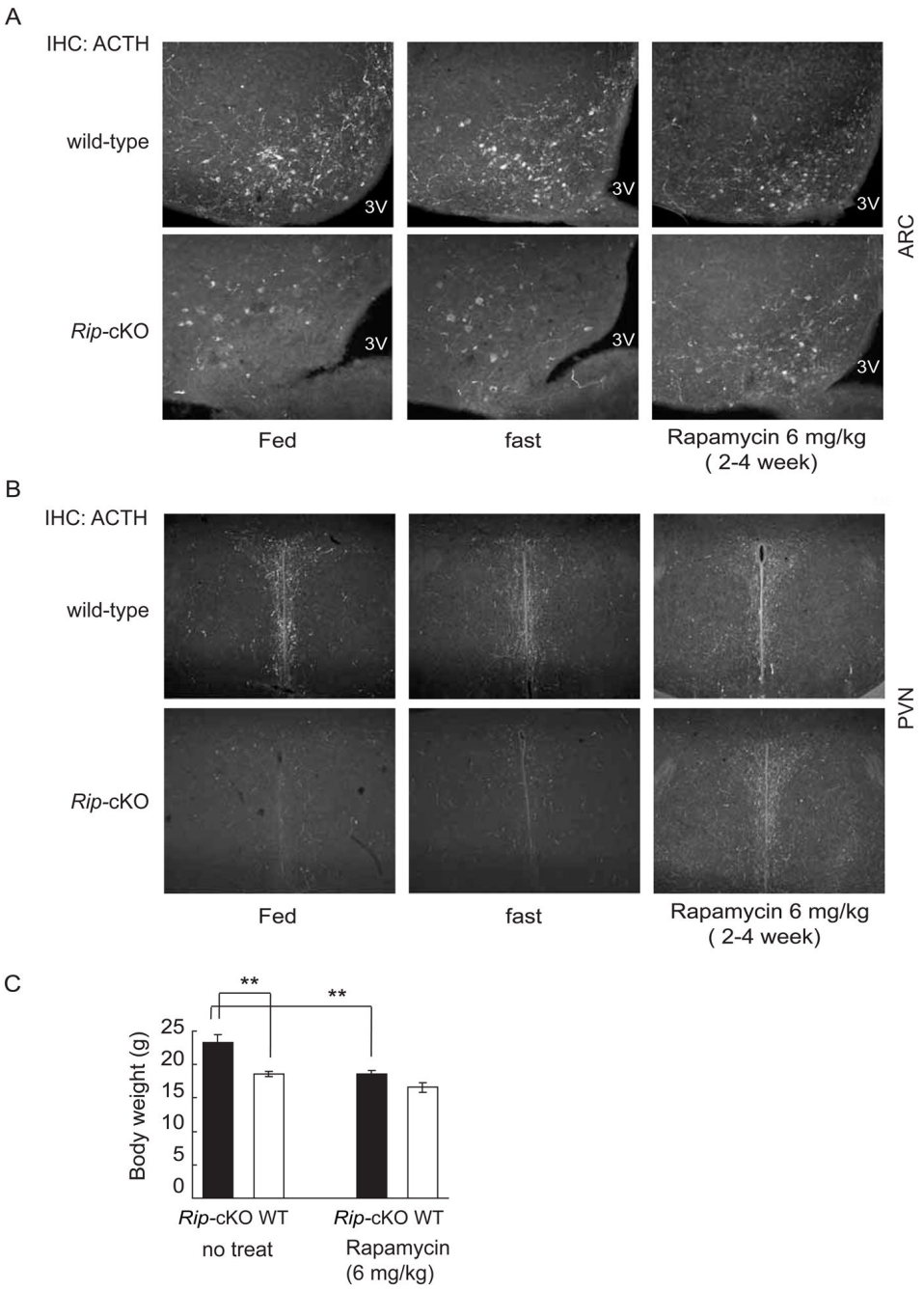

Figure 3. Rapamycin treatment normalized the morphological alterations of Pomc neurons in *Rip-Tsc1*cKO mice

(**A**) Rapamycin normalized the morphological alterations of ACTH-immunoreactivity (IR) cells in the *Rip-Tsc1*cKO arcuate nucleus (ARC), 3V: third ventricle

(**B**) Rapamycin normalized the density of ACTH-IR projections to the PVN in *Rip-Tsc1*cKO mice. PVN: paraventricular nucleus (**A, B**) Representative images of ACTH-IR in *Rip-Tsc1*cKO and wild-type hypothalami. 24-hr-fasted or *ad lib* fed *Rip-Tsc1*cKO and control mice were used for this experiment. Rapamycin samples; 2-week-old *Rip-Tsc1*cKO and control mice were injected rapamycin (6mg/kg body weight) every other day for 2 weeks. The hypothalami were harvested 12 hr after the last treatment of rapamycin.

(**C**) Rapamycin normalized the body weight of *Rip-Tsc1c*KO mice. Body weight of 6-week old female littermates fed on regular chow diet were compared to animals in which 2-week-old *Rip-Tsc1*cKO and control mice were injected with rapamycin (6mg/kg body weight) every other day until 6-weeks of age. Data are expressed as the average ±s.e.m, ***P* <0.01.
For panels (**A**)–(**C**), *Rip*-cKO: *Rip-Tsc1*cKO, WT: control

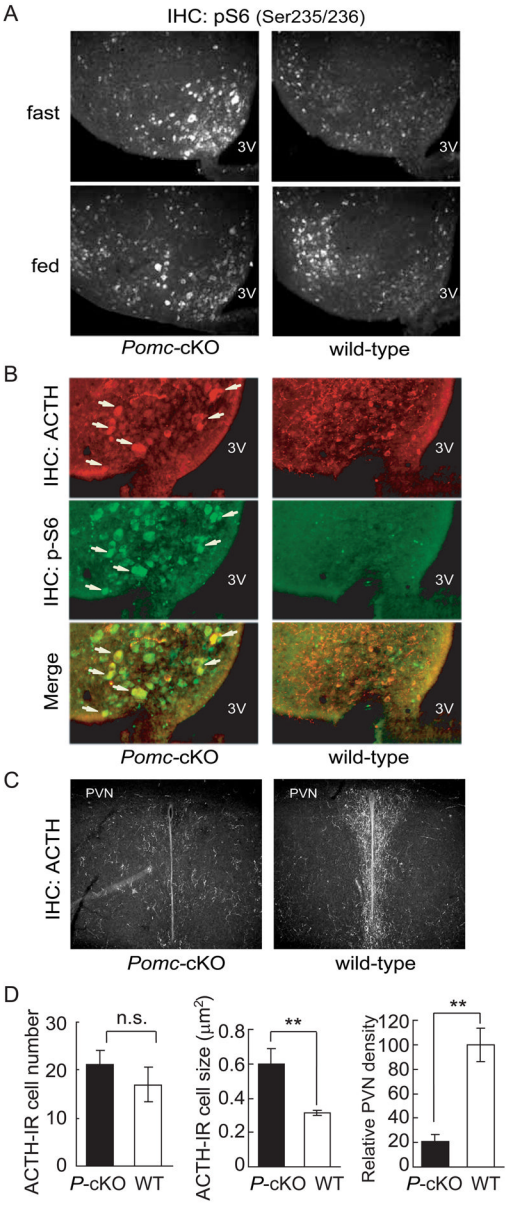

Figure 4. Dysregulation of hypothalamic Pomc neurons in *Pomc-Tsc1*cKO mice

(**A**) *Pomc-Tsc1*cKO mice show increased pS6-immunoreactivity (IR) in the arcuate nucleus. Representative p-S6(Ser235/236) staining of hypothalamus from 4-week old *Pomc-Tsc1*cKO and control mice fasted 24 hr or *ad libitum*-fed.

(**B, C**) Loss of ACTH projections to PVN and increased cell size in *Pomc-Tsc1*cKO mice. Immunohistochemistry for ACTH in hypothalamus of *ad lib* fed 7-week old *Pomc-Tsc1*cKO and control mice, PVN: paraventricular nucleus.

(**B**): Detection of ACTH-IR Pomc neurons (red, upper panel), pS6-IR neurons (green, middle) and their colocalization (lower) in *Pomc-Tsc1*cKO and control animals. Arrows are double-labeled neurons. (**C**): Representative sections of ACTH projections to the PVN.

(**D**): ACTH-IR cell number in arcuate nucleus (ARC), the cell size of the ACTH-IR neurons in ARC and relative projection density in the PVN. ACTH-IR cells from within matched sections were compared with two genotypes as described in Methods (n>7 per genotype) For

PVN projection density, ACTH-IR levels were measured in matched sections and are reported relative to control density. Values are mean ± s.e.m. ***p*<0.01.
For panels (**A**) – (**D**), *P*-cKO or *Pomc*-cKO: *Pomc*-*Tsc1*cKO; WT: control, 3V: third ventricle

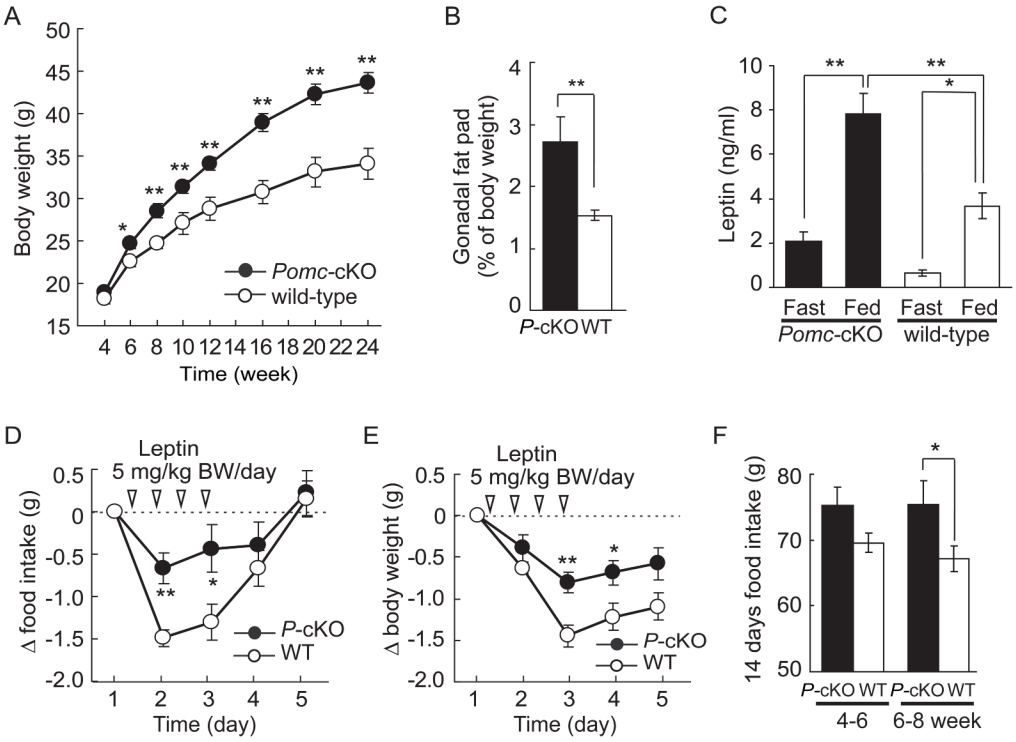

Figure 5. Hyperphagic obesity in *Pomc-Tsc1*cKO mice

(**A**) Obesity in *Pomc-Tsc1*cKO mice. Body weight in male littermates fed on regular chow diet from 4 to 24 weeks of age (KO: $n = 12$, WT: $n = 8$).

(**B**) Increased fat pad in *Pomc-Tsc1*cKO mice. Weight (percentage of body weight) of intra-abdominal fat pad from 8-week old male mice ($n = 7$, male).

(**C**) Hyperleptinemia in *Pomc-Tsc1*cKO mice. Serum leptin levels were measured in 24 hr fasted or *ad lib* fed 4-week old male mice ($n = 6–8$).

(**D, E**) Decreased response to leptin in *Pomc-Tsc1*cKO mice. Mice (4–5 months of age) were injected intraperitoneally with leptin (2.5 mg/kg body weight) twice daily (at 09:30 and 18:30) for 2 days ($n = 6$). (**D**) Changes in food intake are reported relative to baseline intake. (**E**) Body weight was measured every day, and changes are reported relative to initial body weight.

(**F**) *Pomc-Tsc1*cKO mice are hyperphagic. Food intake in male mice over the indicated 2-week periods ($n = 7$).

For panels (**A**)–(**F**), *P*-cKO or *Pomc*-cKO: *Pomc-Tsc1*cKO; WT: control, values are mean ± s.e.m. *$p<0.05$, **$p<0.01$

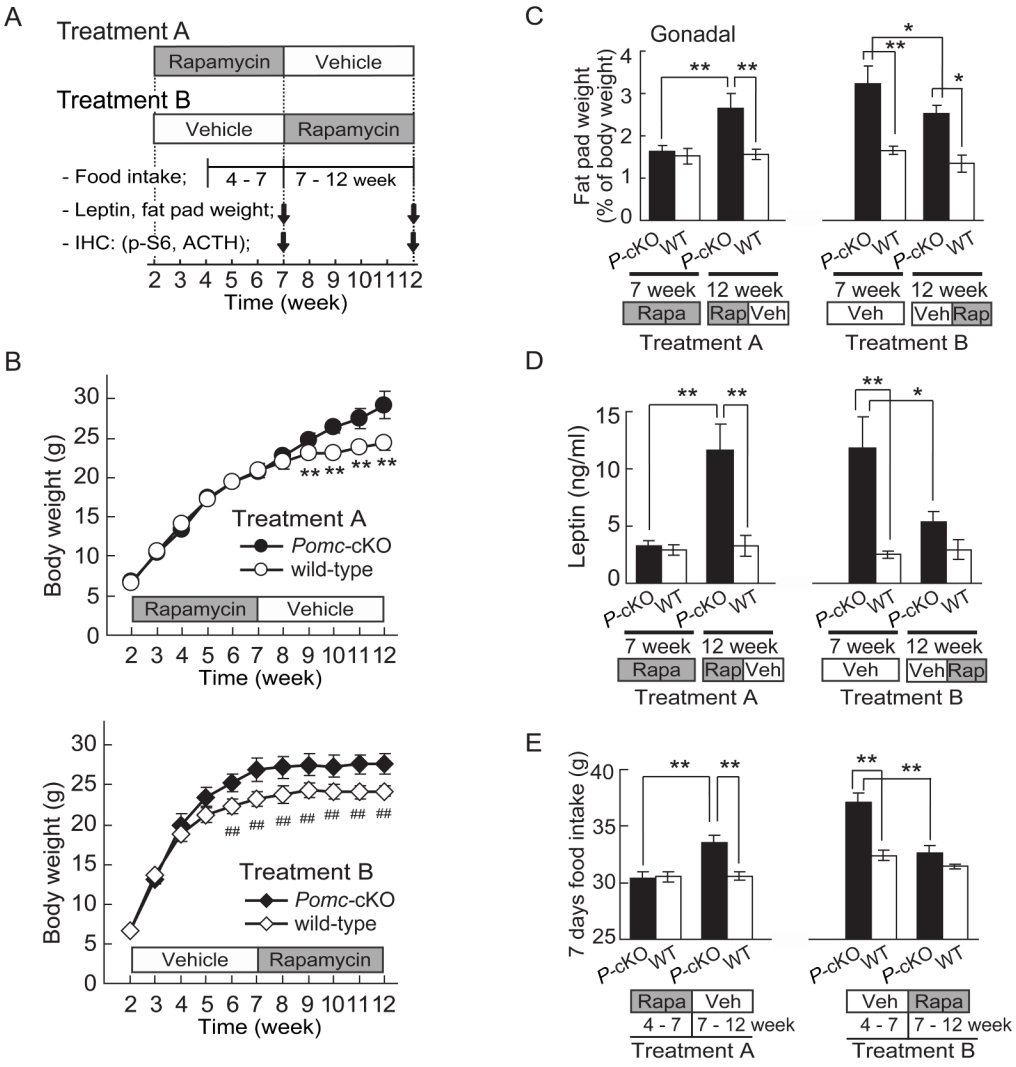

Figure 6. Ongoing rapamycin treatment ameliorates the hyperphagia and obesity of *Pomc-Tsc1*cKO mice

(**A**) Schema of 2 different cohort studies for panels (**B**)–(**H**) and Figure 7 using high dose rapamycin (6mg/kg body weight, i.p. every other day).

Treatment A: *Pomc-Tsc1*cKO and wild-type mice were injected with rapamycin every other day (2–7 week), then injected with vehicle every other day (7–12 week)

Treatment B: *Pomc-Tsc1*cKO and wild-type mice were injected with vehicle every other day (2–7 week), then injected with rapamycin every other day (7–12 week)

(**B**) Rapamycin ameliorated the obese phenotype in *Pomc-Tsc1*cKO mice. Body weight in male littermates fed on regular chow diet from 2 to 12 weeks of age.

Upper panel: Treatment A (n = 6–10)

Lower panel: Treatment B (n = 7–10)

(**C**) Rapamycin normalized adiposity in *Pomc-Tsc1*cKO mice. Weights of gonadal fat deposits (percentage of body weight) from male mice at indicated age (n = 6–10).

(**D**) Rapamycin attenuated hyperleptinemia in *Pomc-Tsc1*cKO mice. Serum leptin levels measured in *ad lib* fed mice at indicated age (n = 6–10).

(**E**) Rapamycin improved hyperphagia in *Pomc-Tsc1*cKO mice. Comparison between weekly food intake in wild-type and *Pomc-Tsc1*cKO mice. Data are average weekly food intake from 4 to 7, or 7 to 12 weeks (n = 6–10).

For panels (**B**)–(**E**), values are mean ± s.e.m. *p<0.05, **p and $^{\#\#}p$<0.01

P-cKO or *Pomc*-cKO: *Pomc-Tsc1*cKO, WT: control**,** Rap or Rapa: rapamycin, Veh: vehicle, Treat.: Treatment

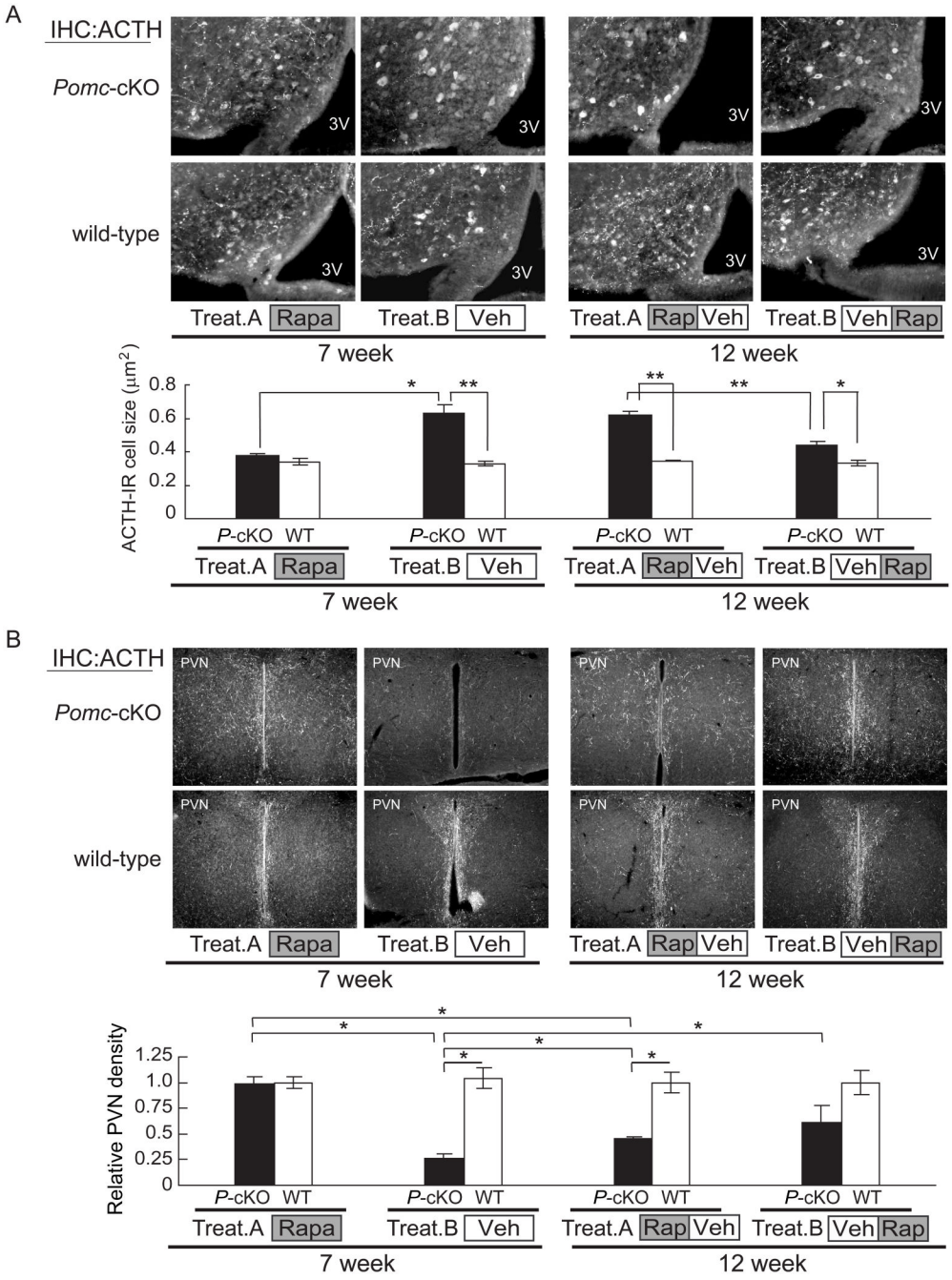

Figure 7. Ongoing rapamycin treatment normalized the morphological alterations of *Pomc-Tsc1*cKO mice

(**A**) Rapamycin normalized the cell size in both young and adult *Pomc-Tsc1*cKO mice. Immunohistochemistry for ACTH in ARC of 7-week (left panels) or 12-week (right panels) old *Pomc-Tsc1*cKO and control mice during Treatment A and B. 3V: third ventricle. (Right panel): Quantification of ATCH-positive cell size in the ARC.

Measurement was as in Figure 4D. n>3 per genotype.

(**B**) Effect of rapamycin on density of PVN projections. ACTH staining of 7- (left panels) and 12-week (right panels) old *Pomc-Tsc1*cKO and control mice following either Treatment A or B. For projection density in the PVN, ACTH stained slices in both genotypes were measured.

Values are expressed relative to projection density of control in each group. PVN: paraventricular nucleus.
For graphs in panels (**A**) and (**B**), values are mean ± s.e.m. **p*<0.05, ***p* <0.01
P-cKO or *Pomc*-cKO: *Pomc-Tsc1*cKO, WT: control**,** Rap or Rapa: rapamycin, Veh: vehicle, Treat.: Treatment